



OPEN ACCESS

EDITED BY

Eduardo Jacob-Lopes,
Federal University of Santa Maria, Brazil

REVIEWED BY

Shaoheng Liu,
Hunan University of Arts and Science,
China
Meifang Li,
Central South University Forestry and
Technology, China

*CORRESPONDENCE

Taiping Zhang,
✉ lckzhang@scut.edu.cn

RECEIVED 15 September 2023

ACCEPTED 25 October 2023

PUBLISHED 08 November 2023

CITATION

Li M, Xiao J, Zeng Z, Zhang T and Ren Y
(2023), Study on the biodegradation of
phenol by *Alcaligenes faecalis*
JH1 immobilized in rice husk biochar .
Front. Environ. Sci. 11:1294791.
doi: 10.3389/fenvs.2023.1294791

COPYRIGHT

© 2023 Li, Xiao, Zeng, Zhang and Ren.
This is an open-access article distributed
under the terms of the [Creative
Commons Attribution License \(CC BY\)](#).
The use, distribution or reproduction in
other forums is permitted, provided the
original author(s) and the copyright
owner(s) are credited and that the original
publication in this journal is cited, in
accordance with accepted academic
practice. No use, distribution or
reproduction is permitted which does not
comply with these terms.

Study on the biodegradation of phenol by *Alcaligenes faecalis* JH1 immobilized in rice husk biochar

Manzhi Li¹, Jiahui Xiao¹, Zhi Zeng¹, Taiping Zhang^{1,2*} and Yuan Ren^{1,2}

¹School of Environment and Energy, South China University of Technology, Guangzhou, China,

²Guangdong Provincial Key Laboratory of Solid Wastes Pollution Control and Recycling, South China University of Technology, Guangzhou, Guangdong, China

Immobilized microbial technology is a sustainable solution to reduce water pollution. Understanding the microorganisms in immobilized biochar is critical for the removal of contaminants in water. Biochar as a carrier of microorganisms, there are some problems need to be focused on, microporous structure blockage limiting the contact between microorganisms and pollutants for further degradation, unstable microbial loading, and low cycle times. To solve these problems, *Alcaligenes faecalis* was immobilized with rice hull biochar to study its adsorption and degradation characteristics of phenol. It was found that *A. faecalis* JH1 could effectively remove 300 mg/L of phenol within 24 h. The adsorption capacity of rice husk biochar for phenol increased with the increasing pyrolysis temperature (700 > 500 > 300°C). The immobilized biomass of JH1 from 700°C rice husk biochar reached 249.45 nmol P/g at 24 h of fixation reaction. It was found that the phenol removal rate of JH1 immobilized at all temperature biochar reached 300 mg/L within 12 h after the sixth cycle. As the number of cycles increased, bacteria grew and adhered to the biochar, forming a thick viscous biofilm and accelerating the removal of phenol. The results showed that *A. faecalis* could firmly adhere to rice hull biochar and degrade phenol effectively, with good durability and cyclicity.

KEYWORDS

biochar, immobilize, bacteria, phenol, mechanism

1 Introduction

Phenol is widely used in various industries (Panigrahy et al., 2022), and the demand for phenol in China ranks third in the world (Zhang et al., 2019). During its manufacturing and usage, a substantial amount of wastewater containing phenol will be released, seriously harming the environment, humans, and other organisms (Mohammadi et al., 2015; Shahryari et al., 2018; Grace Pavithra et al., 2023). The concentrations of these compounds can range from one to several hundred mg/L (Moussavi et al., 2009). It is also listed as a priority pollutant by USEPA (Martínková et al., 2016; Rushing and Santoro, 2022). The treatment methods for phenol wastewater include adsorption (Takaoka et al., 2007), chemical oxidation (Şolpan et al., 2020), biodegradation (Nazos et al., 2020), and so on. Biodegradation is the main way of phenol removal, and its metabolism is mainly controlled by microorganisms through the conversion of phenol into less toxic products

(Iqbal et al., 2018), which considered as an efficient and non-toxic method to treat phenol waste water. Many microorganisms utilize phenol as the sole carbon and energy source which includes both aerobic and anaerobic microorganisms (Panigrahy et al., 2022). However, microbial degradation of phenol is unstable and easy to be affected by environmental factors (Kumar et al., 2005; Usman et al., 2020). Many studies have found that adding shelter for microorganisms can solve the above problems. The synergistic effect of biochar and dominant phenol-degrading strains has been confirmed by relevant studies, and the degradation effect of immobilized microorganisms on pollutants is superior to pure bacteria (Pathak et al., 2018). For example, *Bacillus cereus* SAS19 fixed with porous carbonaceous gel could completely remove 1,600 mg/L phenol within 26 h at the highest. The immobilization of microorganisms effectively improved the survival rate of the strain and the removal rate and speed of phenol (Ke et al., 2018). Sekaran's (Sekaran et al., 2013) research screened and isolated an efficient phenol-degrading bacterium, *Bacillus sp.* 26. The results showed that *Bacillus sp.* 26 immobilized by mesoporous activated carbon had high efficiency in degrading phenol wastewater and excellent recycling performance. In other words, rich pores have a protective effect on microorganisms, improve the tolerance of strains to pollutants, and further enhance the degradation ability of pollutants-degrading bacteria.

With a high level of aromatization, a significant amount of specific surface area, and a well-developed pore structure (Frankel et al., 2016; Zheng et al., 2021), biochar is not only an effective, excellent, and affordable adsorbent but also a good carrier for immobilizing microorganisms. Compared with other carriers, biochar has the advantage of good stability (Shen et al., 2021), which can protect microorganisms from the adverse external environment and improve their tolerance to toxins (Zhao et al., 2020). After it is loaded with microorganisms, it still has strong contact adsorption with pollutants and a good mass transfer effect (Priyadarshini et al., 2023), which is especially suitable for the attachment of microorganisms with a large volume and a fast growth rate. The mechanism of the immobilized microbial method to remove pollutants in water is the synergistic effect of adsorption and biodegradation (Gai et al., 2016; Lyu et al., 2018; Amin and Chetpattananondh, 2019; Huang et al., 2020). The biochar prepared from corn stalk was used to immobilize *Sphingomonas sp.* DZ3 for the 4-Brominated diphenyl ether (BDE-3) removal study. The results showed that biochar had a protective effect on the strain and improved the strain's tolerance to high concentrations of BDE-3 (Du et al., 2016). All of the aforementioned studies indicated that biochar immobilized microorganisms could not only take advantage of the adsorption characteristics of biochar but also offer the dominant species a suitable dwelling environment. Hence, the key benefits of immobilized microbial processes for phenol wastewater treatment include superior removal capabilities, increased resilience to varying environmental conditions, and convenient recuperation and reutilization.

However, we found that the excessive microporous formations within activated carbon led to the occupation of the active sites by microorganisms during the initial stages of immobilization, thereby restricting the interaction between strains and pollutants in the

subsequent reaction phases. This limitation proved unfavorable for pollutant degradation (Toh et al., 2013). During the investigation into the elimination of bisphenol-A from water using microorganisms immobilized on coconut biochar, it was observed that while the removal efficiency of immobilized microorganisms was superior to that of coconut carbon alone, the overall removal rate reached only 59.37%. Furthermore, the microbes exhibited a weak attachment to the biochar substrate and were susceptible to disruption by changes in fluid flow rate within the reactor (Yu et al., 2023). In general, most of the biochar currently studied has disadvantages of low degradation rate of organic pollutants during the immobilization of microorganisms, such as high pyrolysis temperature, limited contact with pollutants after microporous structure of carbon loaded with microorganisms, and unstable adsorption of microorganisms on biochar.

In order to solve the above problems, rice husk biochar will be used as the microbial carrier in this study. Rice is one of the main crops in China, and its output ranks first in the world (Yao et al., 2016). In 2018, the output of waste rice husk reached 1.5×10^{11} kg (Singh, 2018). Which means the carbon raw material of rice husk is easy to obtain and is a good green economic material. Rice husk biochar comes from a wide range of sources and has low cost (Wang et al., 2019; Jjagwe et al., 2021). The excellent specific surface area of rice husk biochar can provide a good adsorption and survival site for dominant bacteria, and the abundant functional groups enable bacteria to bind firmly and further form film to remove pollutants. Then the research focused on the selection of microbial carriers with green environmental protection and high load capacity. Specifically, the effective interactions between pollutants and microorganisms loaded onto biochar for advancing degradation were established. Building upon these challenges, we aimed to conduct recycling experiments on the immobilized microorganism to examine its potential for daily practical application. Therefore, the dominant strain JH1 for degrading phenol was screened by adsorption and immobilization of rice husk biochar prepared at different temperatures (300, 500 and 700°C) as a carrier, and its joint removal effect on phenol was explored, and its immobilization performance was analyzed by recycling. The water-soluble organic carbon of biochar which may influence the bacterial degradation of phenol was also demonstrated. It lays a theoretical foundation for the removal of phenol in practice.

2 Materials and methods

2.1 Domestication, isolation and identification of strains

Domestication: Under aseptic conditions, 30 mL of coking wastewater sludge supernatant was inoculated into 70 mL of sterilized acclimation screening medium (S1) containing 100 mg/L of phenol. The mixture was then cultured for 2–7 days under aerobic oscillation at 30°C and 150 rpm. Afterwards, the 30 mL of oscillating medium was transferred into 70 mL of acclimated screening medium with 200 mg/L of phenol, and the culture was continued under the same conditions for 2–7 days. Following this method, the process was repeated four times, the concentration of

phenol was gradually increased in the inorganic salt medium to 300, 500, 800, and 1,000 mg/L, respectively. The domestication process lasted for six cycles.

Isolation and identification: The mixed bacteria were separated using the dilution coating plate method. For the final cycle of acclimation, the acclimation screening medium with a phenol concentration of 1,000 mg/L was prepared and plated. A gradient-diluted bacterial solution of 1 mL was evenly spread on an LB medium (S1) plate containing agar and incubated inverted in a constant-temperature incubator at 30°C for 2 days. Colonies of JH1 were selected and purified on the plate, and they were sent to Hangzhou Yanqui Information Technology Co., Ltd. For identification. The JH1 strain was then enriched and cultured in LB medium. Subsequently, 100 mL of MSM medium (S1) containing 150 mg/L of phenol was added to a conical bottle at a concentration of 1.2×10^8 CFU/mL and cultured at 30°C and 150 rpm for 12 h. Strain JH1 was selected for testing its performance in phenol degradation.

2.1.1 Results of phenol-degrading bacteria

After the above domestication, isolation and phenol degradation experiment for 12 h, the dominant strain JH1 was shown in [Supplementary Figure S1](#). The colony appearance was milky white, round, with leafy edges, translucent, and radial folds on the surface. Strain JH1 was enriched and cultured in LB medium for 24 h, and the bacterial solution and glycerol (1:1) were stored, and this strain was selected for subsequent experiments.

2.1.2 Analysis of 16S rDNA sequence of strain JH1

The sequence information (S2) obtained by sequencing was input into the Blast comparison system of NCBI data, and the sequence was compared with the known sequences in NCBI to obtain a sequence with high homology. Then MEGA7.0.14 software was used to construct the phylogenetic tree, as shown in [Supplementary Figure S2](#). According to phylogenetic tree, strain JH1 belonged to *Alcaligenes*, and its closest relative strain was *Alcaligenes faecalis strain IAM 12369*, and the rDNA similarity of 16S is 99.2%. Therefore, strain JH1 was identified as *A. faecalis*.

2.2 Experiments on the growth curve and phenol degradation kinetics of strain JH1

Bacteria solution (6×10^7 CFU/mL) were added to 100 mL MSM medium with 300 mg/L phenol and cultured at 30°C, pH 7.0 and 150 rpm with light shock. The samples were collected at 0, 1.5, 3, 4, 6, 8, 10, 12, 14, 16, 20 and 24 h while the control group was MSM medium containing only 300 mg/L phenol at the same time, so as to exclude the loss of volatilization and natural degradation. After centrifugation at 6,000 r/min for 10 min, the concentration of phenol in 1 mL supernatant was determined through a Gas Chromatography-Flame Ionization Detector (GCMS-QP2010 Ultra, Shimadzu, Japan).

The bacterial concentration was determined using the optical density method, where the light absorption value of the bacterial solution was measured at a wavelength of 600 nm. The growth curve experiment of strain JH1 is shown in the ([Supplementary Material S3](#)).

2.3 Preparation and characterization of biochar

Biochar was prepared from waste rice husks rich in minerals. The dried rice husks were crushed by a high-speed multifunctional crusher and passed through a 12.7-mesh sieve, then transferred to a quartz boat in a tube furnace, and pyrolyzed for 2 h at a heating rate of 5 C/min under anoxic conditions. The pyrolysis temperatures were 300°C, 500°C and 700°C, respectively. After pyrolysis and cooling to room temperature, the rice husk biochar (D3, D5, D7) was ground through a 100-mesh sieve, washed with deionized water, and baked in an oven at 80°C for 12 h. The biochar was prepared into a sealed bag and stored in a dryer for later use.

The percentage content of C, H, N and S elements in biochar was directly determined by elemental analyzer (UNICUBE, Elementar, Germany). The micromorphology of biochar was analyzed by high-resolution field emission scanning electron microscopy (Merlin, Zeiss, Germany). The specific surface area and pore size were determined by a fully automatic specific surface and porosity analyzer (ASAP 2460, MAC, United States) using N₂ adsorption-desorption isotherm test (BET). X-ray diffractometer (Empyrean, Panaco, Netherlands) was used to analyze the crystal structure of biochar prepared under different raw materials and different temperature conditions. Fourier infrared spectroscopy (Nicolet is50, Thermo Scientific, United States) was used to analyze the surface functional groups of biochar and adsorbed phenol.

2.4 Study on adsorption properties of phenol by biochar

2.4.1 Adsorption kinetics experiment

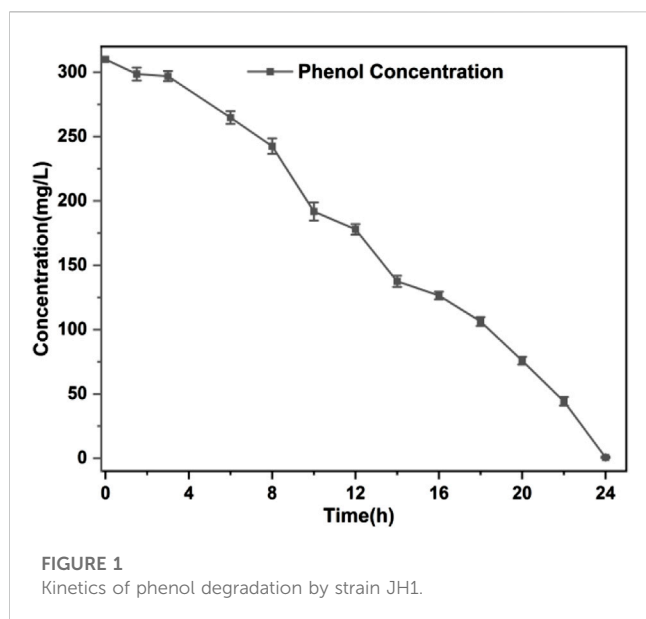
The adsorption experiment of phenol was carried out at 30°C and 150 rpm. 0.02 g of three kinds of biochar were added into 10 mL phenol solution with a concentration of 300 mg/L and a pH of 7, respectively. Samples were taken at 0, 1.5, 3, 4, 8, 12, 24, 36 and 48 h of adsorption. The biochar was separated from the solution using 0.45 μm organic filter. The residual phenol concentration was determined and the equilibrium adsorption capacity of each carbon was calculated.

2.4.2 Adsorption isotherm experiment

The isotherm experiment of phenol adsorption by biochar was similar to the kinetic investigation, except that the initial concentration of phenol was 50, 100, 200, 400, 600, 800 and 1000 mg/L, and other experimental conditions and test methods were consistent. Samples were taken 24 h after adsorption. For details, see [Supplementary material S4](#).

2.5 The preparation of immobilized biochar by strain JH1

Strain JH1 was cultured in LB medium at 30°C and 150 rpm in a shaking table for 24 h, centrifuged at 5,000 r/min after culture. The bacteria was cleaned with PBS, collected, and re-suspended into a solution with OD₆₀₀ = 1.0, i.e., which density was 1.2×10^9 CFU/mL. Biochar and strain JH1 cell suspension were mixed at a ratio of



5:100 (W/V), oscillated in a full-temperature culture shaker at 30°C and 150 rpm for 24 h, the bacteria on the surface of biochar was adsorbed and fixed, and then centrifuged at 1,000 r/min for 10 min. The supernatant was filtered out and air dry at room temperature. Three of the immobilized bacterial biochar were named JD3, JD5 and JD7, respectively.

For the determination of JH1 biomass on biochar, see [Supplementary Material S5](#).

2.6 Research on the performance of recycling

0.5 g of biochar in [Section 2.6](#) was placed in 50 mL MSM medium containing 300 mg/L phenol under the same culture conditions as in [Section 2.2](#). The concentration of phenol in the solution was measured periodically, and its removal rate was calculated. When the degradation rate of phenol in the solution reaches 99%, the first cycle ends. The conical bottle was left for 1–2 min. After the biochar was precipitated, the supernatant was extracted with a syringe, and then 50 mL of the newly prepared 300 mg/L phenol solution was added. The process was repeated for 8 cycles.

3 Result and discussion

3.1 Phenol degradation kinetics curve of strain JH1

The bacterial growth curve ([Supplementary Figure S3](#)) could clearly show the delayed, logarithmic and stable stages of phenol degrading bacteria. In LB liquid medium, strain JH1 entered a logarithmic stage after 3 h, a logarithmic stage during 3–14 h, and a stable stage after 14 h. For MSM medium, the phenol-degrading bacteria entered the logarithmic stage after 3 h, and then they grew slowly until the number of bacteria in the medium reached the maximum at 24 h, but the number of

bacteria in the stable stage was less than one-quarter of that in LB liquid medium.

The degradation curve of strain JH1 to phenol was shown in [Figure 1](#). Due to the delayed growth phase of strain JH1, the rate of phenol degradation in the first 3 h was low. After 3 h, the bacteria multiplied and grew quickly using the remaining LB medium and phenol in the solution, and the phenol content gradually declined. After 24 h, strain JH1 degraded phenol at a rate of 99%.

3.2 Characterization of biochar

[Table 1](#) illustrated the yield, element composition, and element content ratio of rice husk biochar prepared at different temperatures. As the temperature increased, the biochar production from rice husk decreased due to the faster breakdown of biomass into volatile substances and biochar during pyrolysis, leading to a lower volatile content ([Liu et al., 2015](#)). However, once the carbonization temperature reached 700°C, the content of volatile substances and the yield of biochar stabilizes ([Keiluweit et al., 2010](#); [Ahmad et al., 2016](#)). The content ratio of each element could be utilized to describe the physical and chemical properties of biochar. Specifically, the ratios of O/C, H/C, and (O + N)/C respectively indicated the stability, aromaticity, and polarity of biochar ([Rutherford et al., 2012](#); [Sun et al., 2013](#); [Guo and Chen, 2014](#); [Park et al., 2015](#)). These ratios suggested that the surface of rice husk biochar contains a higher amount of oxygen and nitrogen functional groups, which might facilitate the adsorption and growth of microorganisms, and exhibited more active functional groups compared to coal ([Palansooriya et al., 2020](#)). Consequently, it could enhance the active attachment of microorganisms ([Zhang et al., 2014](#)).

Scanning electron microscopy (SEM) was used to observe the morphology and structure of rice husk biochar, as shown in [Figure 2](#). As we can see, with the increase of carbonization temperature, the pore and channel structure of biochar became more and more obvious. This structural property could provide a suitable habitat for microbial attachment and proliferation, and the porous structure was also conducive to the adsorption of pollutants.

In this investigation, the test results of specific surface area, pore capacity and average pore diameter of rice husk biochar were shown in [Table 2](#). The observation indicated that as the pyrolysis temperature rose, the specific surface area and pore capacity of rice husk biochar exhibited a growth, whereas the average pore size decreased. The collected data demonstrated that mesoporous structures ranging from 2 to 50 nm were predominantly found in D3 and D5, whereas D7 possessed an average pore size similar to micropores. As the pyrolysis temperature rose, the specific surface area of biochar increased ([Balmuk et al., 2023](#)), leading to improved contact opportunities with pollutants and offering more sites for bacteria attachment and growth.

3.3 Study on the adsorption properties of phenol by biochar

3.3.1 Adsorption kinetics

The simulation curve for phenol adsorption kinetics of biochar was shown in [Figure 3A](#). As described in Eqs 1, 2 of [S6](#), the adsorption

TABLE 1 The yield, chemical composition and element content ratio of biochars.

Biochar Sample	Yield (%)	Chemical composition (%)					Element content ratio		
		C	H	O	N	S	O/C	H/C	(O + N)/C
D3	51.50	47.24	3.894	48.242	0.527	0.097	1.021	0.082	1.032
D5	37.90	49.08	2.207	48.064	0.526	0.123	0.979	0.045	0.990
D7	35.50	50.25	1.163	48.237	0.350	0.000	0.960	0.023	0.967

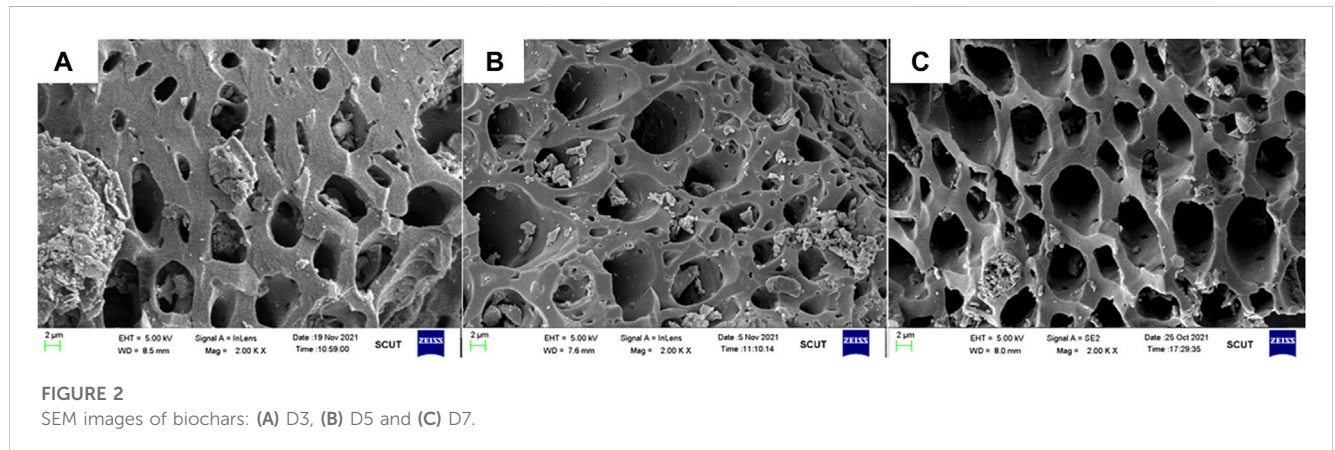
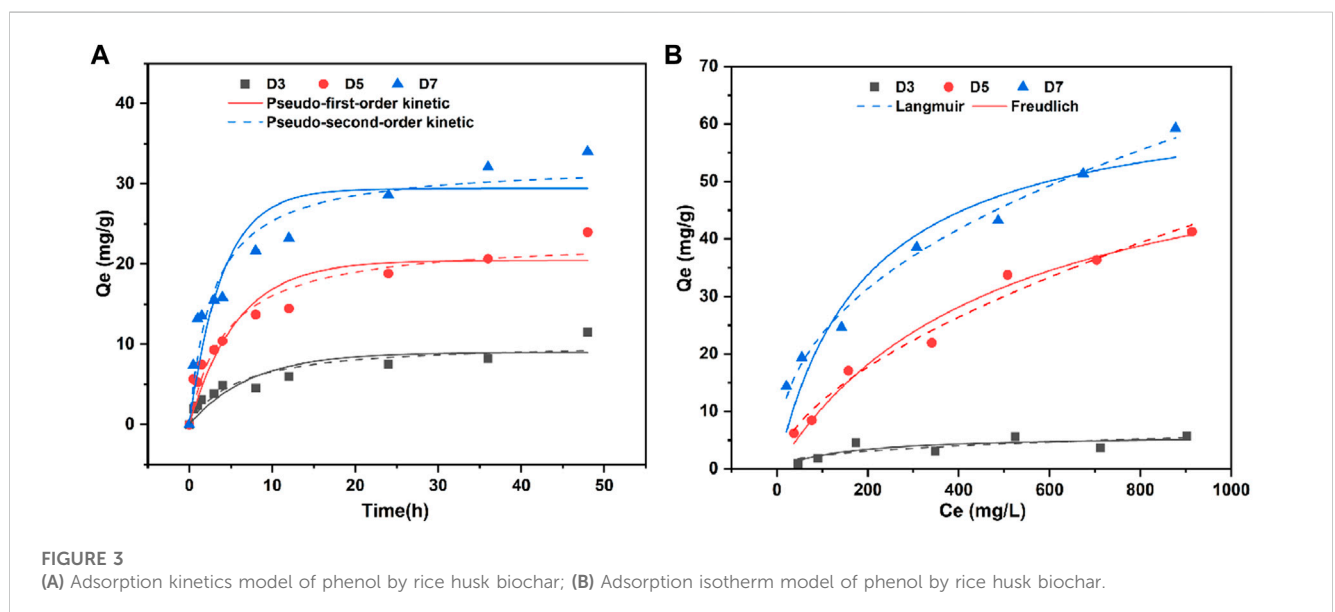


TABLE 2 The pore structure parameters of biochars.

Biochar sample	BET (m ² /g)	Pore capacity (cm ³ /g)	Average aperture (nm)
D3	1.9558	0.003939	8.0552
D5	33.4325	0.027041	3.2353
D7	217.6638	0.106998	1.9663

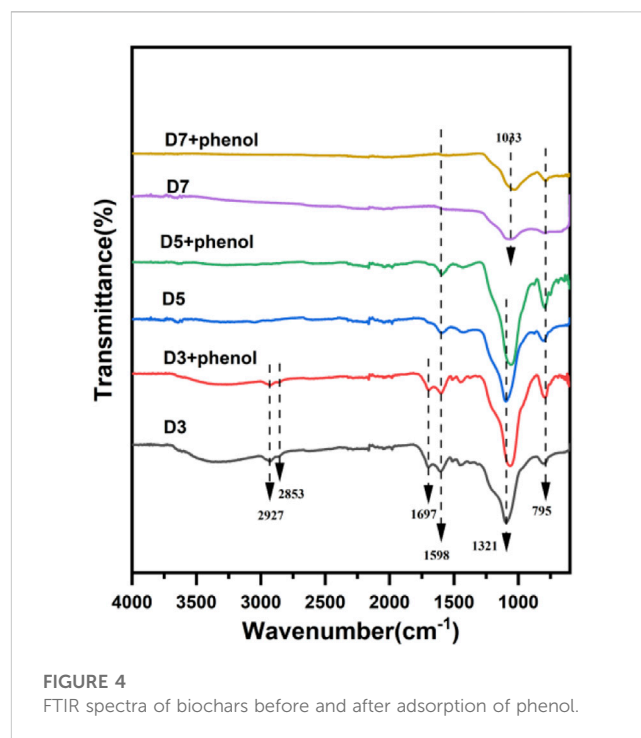


kinetics of phenol by biochar were evaluated using the pseudo-first-order and pseudo-second-order kinetic models. Initially, the rate of phenol adsorption by biochar increased rapidly with longer contact time, but eventually decreased until reaching equilibrium after approximately 8 h. This decline may be attributed to the saturation of available binding sites on the biochar. [Supplementary Table S1](#) presented the parameters obtained from curve fitting. The pseudo-second-order kinetic coefficients exhibited higher R^2 values compared to the pseudo-first-order kinetic coefficients for all three types of carbon. Additionally, the error in the saturation adsorption capacity of the pseudo-second-order kinetic equation was lower than that of the pseudo-first-order kinetic equation. The results indicated that the adsorption capacity of biochar primarily relied on its surface active sites, thus suggesting that the pseudo-second-order kinetic model provides a better characterization of the phenol adsorption process on biochar. The adsorption process was chemical adsorption (Li et al., 2023), and phenol could be chemically adsorbed to the surface of biochar (Zhao et al., 2019).

Figure 3B showed the isotherm model of adsorption of phenol by rice husk biochar. Langmuir model and Freundlich model were used to describe the adsorption process of phenol by biochar, as shown in equation S7 (3) and (4). With the increase of the initial phenol concentration, the adsorption capacity of biochar for phenol increased, but when the phenol concentration was greater than 300 mg/L, the adsorption equilibrium of biochar was reached. The parameters obtained after fitting the curve model were shown in [Supplementary Table S2](#). Both Langmuir and Freundlich models fitted the data well. Among them, the R^2 coefficient of the Langmuir model of D3 biochar was higher than that of the Freundlich model, and the Langmuir model assumed that the adsorption is homogeneous, so D3 was a single molecular layer adsorption process, that is, once phenol occupied the binding site, no further adsorption could occur at this site (Du et al., 2016). The R^2 coefficients fitted by the Freundlich model of the other two kinds of biochar were all higher than those fitted by the Langmuir model. Therefore, the fitting effect of the Freundlich model was better than that fitted by the Langmuir model. The Freundlich isotherm assumed a heterogeneous surface with non-uniform distribution, which indicated that D5 and D7 biochar were more prone to multilayer adsorption. The n value of Freundlich isothermal model represents the adsorption strength. Generally, the larger n is, the easier the adsorption process is. When $0.1 < 1/n < 1$, indicated that it was easy to adsorb pollutants (Tong et al., 2019). All the n in the fitting results of this study belong to the range of $0.1 < 1/n < 1$, which indicated that the adsorption of phenol on biochar was easy and the adsorption effect was good. According to the fitting parameters of Langmuir model, the maximum adsorption capacity of D7 in rice husk biochar prepared at different temperatures was the largest, reaching 66.02 mg/g.

3.4 Characterization of phenol adsorption by biochar

[Supplementary Figure S4](#) was the scanning electron microscope image magnified by 5 k after adsorption of phenol by rice husk carbon. After adsorption of phenol by biochar, the surface structure of biochar showed obvious changes compared with that before adsorption (Figure 2). The presence of a significant quantity of granular material



resulted in the transformation of the initially smooth surface of biochar into a rough and wrinkled texture, leading to a tighter interconnection between biochar structures. This change is likely attributed to the substantial adsorption of phenol on the biochar surface.

In order to further verify the adsorption of phenol by biochar, the biochar before and after the adsorption of phenol was analyzed by Fourier infrared spectrometer. As shown in Figure 4, the peak values of rice husk biochar at 2,927 and 2,869 cm^{-1} belonged to aliphatic $=\text{CH}_2$ groups (Shen et al., 2017). At 1,698 cm^{-1} , the $=\text{C}=\text{O}$ tensile vibration of carboxyl group was observed, and the absorption peak decreased after the pyrolysis temperature of 500°C. $\text{C}=\text{C}$ in aromatic hydrocarbons appeared about 1,590 cm^{-1} , and the peak strength of $\text{C}=\text{C}$ became weaker and weaker with the increase of pyrolysis temperature, because the degree of condensation increased at higher carbonization temperature (Keiluweit et al., 2010). With the increase of pyrolysis temperature, the absorption peak of $\text{C}=\text{C}$ (1,512 cm^{-1}) of lignin gradually decreased from 300°C to 500°C, and even disappeared at 700°C. The peak around 1,300 cm^{-1} was caused by the stretching vibration of the ether functional group ($\text{C}-\text{O}-\text{C}$) (Yang et al., 2019), and also only occurs at a low temperature of 300°C. With the increased of pyrolysis temperature, these peaks became less or even disappear, which represented the organic content of biochar decreased with the increased of pyrolysis temperature (Fan et al., 2023).

Biochar was highly aromatic and porous, and could form $\pi-\pi$ interaction with phenol through the aromatic $\text{C}=\text{C}$ bond or fill phenol through pores (Du et al., 2016). The comparison of FTIR before and after adsorption showed that the spectral band at 1,029 cm^{-1} of biochar attributed to cellulose $\text{C}-\text{O}-\text{C}$ (Xiao et al., 2014), and the absorption peak became significantly narrower and sharper after adsorption of phenol. The $-\text{OH}$, $=\text{C}=\text{O}$, $-\text{CH}_3$ and $\text{C}-\text{O}-\text{C}$ of biochar have stretching vibration changes, so there was hydrogen bonding or electrostatic adsorption. Meanwhile,

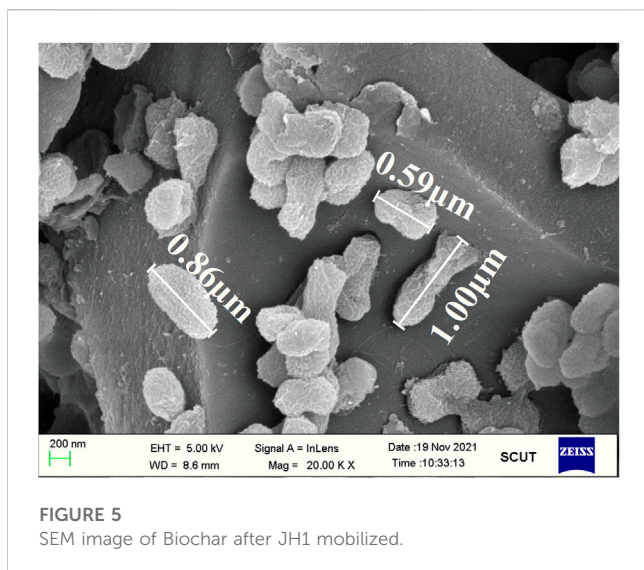


FIGURE 5
SEM image of Biochar after JH1 mobilized.

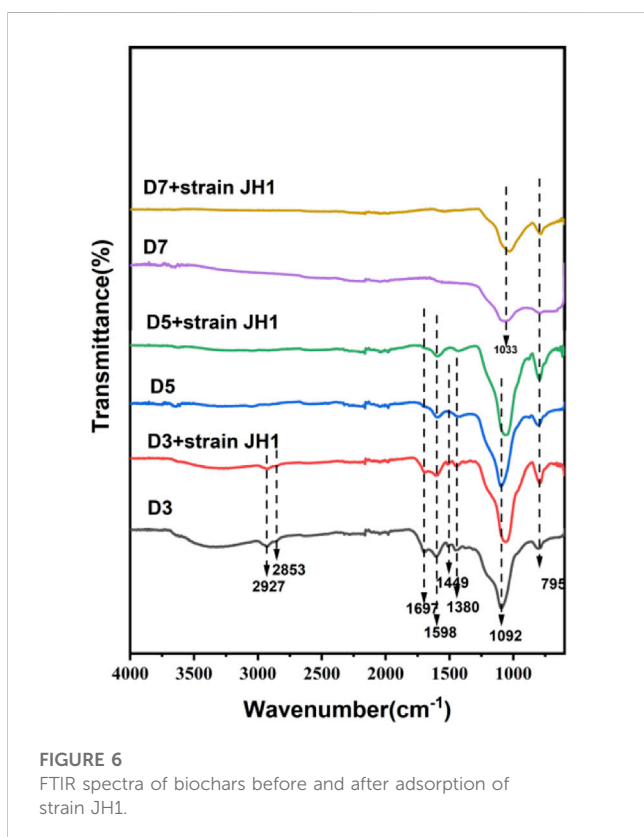


FIGURE 6
FTIR spectra of biochars before and after adsorption of strain JH1.

the benzene ring of phenol was a hydrophobic group, so there was also hydrophobic effect (Wang et al., 2023).

3.5 Studies on biochar adsorption and immobilization of bacterial strains

According to the SEM images of Figure 5, the *A. faecalis* JH1 was short rod-like in appearance, with a length of about 0.5–1.0 μm, and

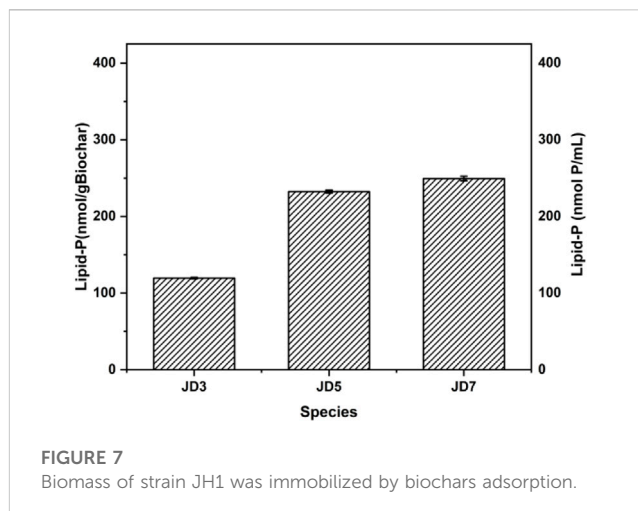


FIGURE 7
Biomass of strain JH1 was immobilized by biochars adsorption.

a large amount of JH1 was anchored on the surface and internal pores of biochar.

The extracellular polymer (EPS) secreted by the bacterial surface will accelerate the secretion when the strain attaches to the carrier, so that the strain will stick firmly to the carrier (Chen et al., 2016). Supplementary Figure S5 showed the FTIR spectrum of strain JH1. Different bands in the figure showed the characteristic peaks of the bacteria. In the proteome, Amide I ($=C=O$) was located at $1,635\text{ cm}^{-1}$, and Amide II (N-H or C-N) was located at $1,530\text{ cm}^{-1}$. The absorption peaks of $1,450\text{--}1,230\text{ cm}^{-1}$ belonged to amino acids in peptidoglycan and $=C=O$ in fatty acids (Dave and Dhayal, 2017). The bands appearing in the range of $1,200\text{--}900\text{ cm}^{-1}$ belonged to the complex vibration of polysaccharide. Aromatic ($-CH$) partially peaked at 854 cm^{-1} .

According to the FTIR diagram before and after biochar adsorption of strain JH1 (Figure 6), the interaction between strain JH1 and different biochar samples was slightly different. The rice husk biochar (D3 and D5) prepared at low temperature showed significant difference in the mixing region of protein and fatty acid ($1500\text{--}1200\text{ cm}^{-1}$) before and after adsorption of strain JH1, while the change trend of D7 was not obvious. $1,200\text{--}900\text{ cm}^{-1}$ belonged to the polysaccharide in the cell wall (Zhu, 2018), and all biochar exhibits obvious stretching vibration. Therefore, FTIR analysis showed that strain JH1 can adhere to the surface of biochar by secreting polysaccharides or proteins. Proteins and polysaccharides in EPS played a key role in promoting initial adhesion and the development of biofilms (Li et al., 2019). The hydrophobicity degree obtained by bacteria on the matrix would affect the number of cells attached to biochar, and the hydrophilicity/hydrophobicity on the surface of biochar would also affect the adhesion ability of bacteria. For example, the presence of fatty acid $-CH_2$ on the surface of bacteria will make bacteria selectively adhere to biochar with stronger hydrophobicity (Ramos-Escobedo et al., 2016). The adsorption of D7 on bacteria mainly relied on hydrophilic groups such as bacterial exopolysaccharides and had strong binding effect (Amenaghawon et al., 2021), such as C-O, $-COO^-$, $=C=O$ and functional groups of aromatic Ar-H (Yu et al., 2019). D3 and D5 had many hydrophobic and hydrophilic groups on the surface, and their adsorption of

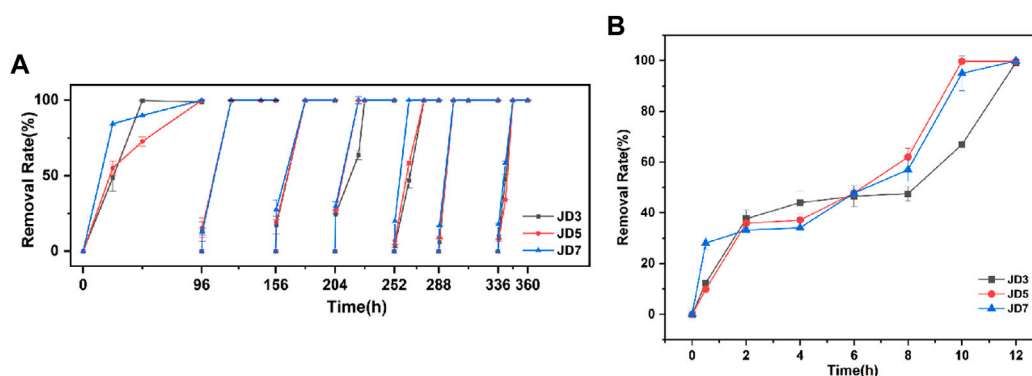


FIGURE 8
(A) Biochars immobilized bacteria for recycling; (B) Phenol removal kinetics curve at eighth cycle.

bacteria was the joint action of bacterial extracellular proteins and polysaccharides.

Figure 7 showed the biomass of three kinds of biochar adsorbed and fixed strains JH1 for 24 h. D7 had the highest fixed biomass within 24 h, which was 249.45 nmol P/g biochar, while D3 had the lowest fixed biomass (D7>D5>D3). The immobilized biomass of biochar may be related to the differences in surface structure and functional groups of the biochar. Combined with FTIR analysis, the abundant hydrophilic groups of 700°C rice husk biocarbon were more conducive to the adsorption of JH1 in a short time and promote the secretion of EPS. The fixed biomass of bamboo charcoal decreased with the decrease of carbon particle size (25 mesh >35 mesh >80 mesh), and the maximum fixed biomass of 80-mesh bamboo charcoal was only 228.26 nmol P/g. The analysis results indicated that the fixed biomass might be affected by affecting bacterial activity (Bakina et al., 2021). The immobilized microorganisms in peanut shell biochar prepared by embedding method showed that the specific surface area of the material loaded with microorganisms was 26 times smaller than that of the original biochar, and the pollutants in the water needed ion diffusion to reach the inside of the biochar before they could be utilized by bacteria, which was not conducive to the activation and growth of the strain, resulting in the strain easily falling off later (Wu et al., 2021). The cyclic removal experiment was carried out to investigate the removal effect of phenol after immobilized microorganism of rice husk biochar.

3.6 Recycle experiment of biochar immobilized bacteria

As depicted in Figure 8A, the results of the biochar immobilization of JH1 demonstrated that the rate of phenol removal in the first cycle (1C) process was slower compared to other cycles. However, as the number of cycles increased, the rate of phenol removal became faster. This can be attributed to the rapid reproduction, growth, and adhesion of bacteria on biochar due to the phenol adsorption by biochar and the presence of nutrients within biochar itself. Consequently, the number of bacteria on biochar increased, resulting in a shorter time required for the

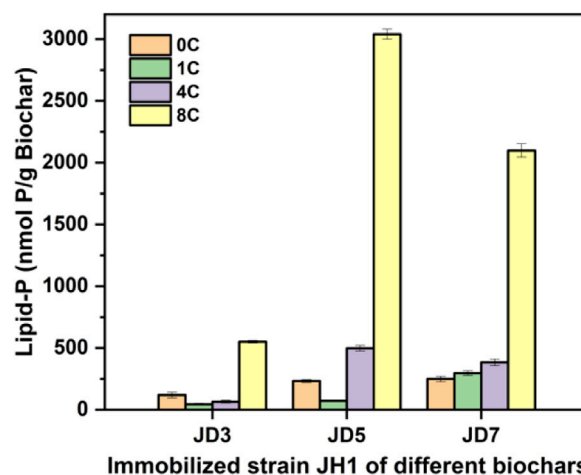


FIGURE 9
Biomass of biochars immobilized strain JH1. Annotation: 0C, 1C, 4C, 8C indicated none cycle, first cycle, fourth cycle and eighth cycle.

removal of phenol from the solution by biochar-immobilized bacteria. After the sixth cycle, biochar-immobilized bacteria at all temperatures were capable of removing up to 300 mg/L of phenol solution within 12 h.

Figure 9B illustrated the experiment involving the eighth cycle (8C) of biochar solidified strain JH1. The findings indicated that during the initial reaction stage, JD7 exhibited a faster and more significant removal of phenol compared to JD3 and JD5. However, in the final stages, JD5 exhibited a slightly higher removal rate of phenol than the other two strains. Taking into account the analysis presented in Figure 3A, while keeping all reaction conditions uniform, it could be inferred that the phenol removal capacity of JD7 at the initial stage of the reaction was 82 mg/L, whereas the phenol removal capacity of rice hull biochar was 29 mg/L. This suggested that the removal of phenol by JH1-fixed biochar was primarily due to the adsorption of phenol by biochar, followed by subsequent bacterial degradation.

To further explain this phenomenon, the biomass of biochar immobilized bacteria at 1°C, 4°C and 8°C was measured, including

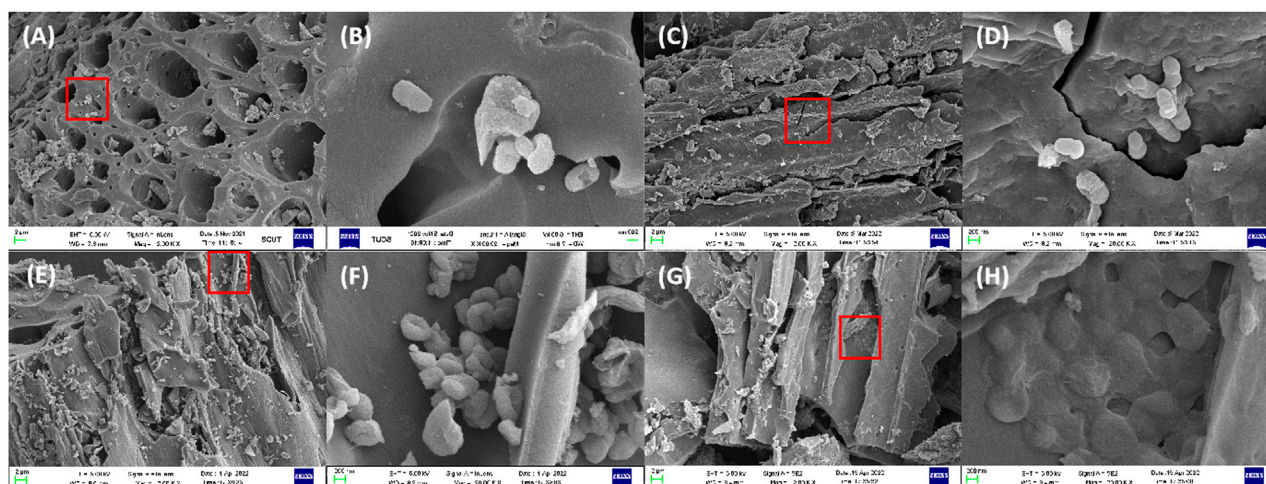


FIGURE 10

SEM images of different cycles: (A) and (B) 0C, (C) and (D) 1C, (E) and (F) 4C, (G) and (H) 8C. Annotation: 0C, 1C, 4C, 8C indicated none cycle, first cycle, fourth cycle and eighth cycle.

the biomass of biochar fixed bacteria before recycling (0C), as shown in Figure 9. After 1C, the biomass of both JD3 and JD5 decreased compared to 0C, indicating that the bacteria were not stably adsorbed on the biochar and were re-suspended into the solution during usage. This finding also explains why 1C phenol removal rates and rates were slower than those of other cycle batches. In the process of recycling, the number of bacteria on the three kinds of biochar all increased and reached the maximum value at 8°C. The biomass of JD5 was the highest among all the biochar immobilized bacteria. It was 2,634.18 nmol P/g biochar, which was consistent with the results of the above 8°C cycle experiment. At 8°C, rice husk biochar prepared at 500°C has the highest number of fixed bacteria comparing with other two. This was because the adsorption force may also depend on the pore size, and if microorganisms are to enter the pore, the optimal pore size for adsorption may need to be 2 to 5 times larger than the cell size (Lehmann et al., 2011), with a length of about 0.5–1 μm for the *A. faecalis* JH1 (Figure 5), the most suitable pore size should be 1–5 μm. Therefore, the micropore structure in D7 has an impact on the continued adsorption of more cycles after loading a large number of bacteria, the large pore size of D3 is not conducive to the adsorption of JH1. So the pore size and pore curvature of D5 are most suitable for the growth of JH1 strain. Hence, according to Figure 8B, JD5 in the 8°C cycle experiment was more conducive to the adhesion of strain JH1 and the subsequent removal of phenol adsorbed by biochar because of its more suitable pore size. The overall results showed that rice husk biochar was a good biological carrier of JH1, which was conducive to the growth and immobilization of bacteria.

Figure 10 showed SEM images of different cycles. (a)–(h) are 2 k× and 20 k× multiples of 0°C, 1°C, 4°C and 8°C in the cycle, respectively. The image directly showed that with the repeated replacement of phenol, the bacteria adhering to the surface of biochar make use of the phenol adsorbed by biochar, split with a single bacterium as the center, multiply around it, and became a multi-bacterial community. In the eighth cycle, a thick and sticky biofilm was established on the surface of biochar, as shown in

Figures 10G, H. In the presence of phenol, microorganisms secrete more extracellular polymers (EPS) to form biofilms, which cover the surface of microorganisms (Zeng et al., 2021) and protect them from the toxicity of high-concentration pollutants (Huang et al., 2020). When the thickness of the biofilm is 10–20 μm, both phenol and oxygen can diffuse into the interior of bacteria for metabolic activities (Wang et al., 2015). The SEM images of the three biochar fixed strains JH1 were basically the same, and the growth and adhesion of bacteria on biochar showed such a change rule.

These results indicated that the long-term removal of phenol by biochar solidified bacteria JH1 depended more on the biodegradation than on the simple adsorption process. Biochar prepared under suitable conditions was an ideal biological carrier, with a large specific surface area for bacterial adhesion and growth, in addition, it was beneficial to transport oxygen and substrate through the immobilized cells, and enhance the activity of the immobilized bacteria. Biochar immobilized JH1 had great potential for phenol removal and is reusable, showing good stability and durability, which was consistent with the results of most recycling studies (Liu et al., 2012; Qiao et al., 2020).

4 Conclusion

In this paper, we had domesticated and isolated the dominant strain of metabolizing phenol in coking wastewater, alkaline *Alcaligenes Faecalis* JH1, and studied the degradation characteristics of the bacteria. It was found that JH1 had a good degradation effect on phenol. Under the conditions of 6×10^7 CFU/mL, 30°C, pH = 7 and salinity less than 1%, the removal rate of 300 mg/L phenol could reach 99% within 24 h. Rice husk biochar (D3, D5, D7) had a porous structure, and the specific surface area increased with the increase of temperature, which increased the adsorption capacity of phenol. According to adsorption kinetics and adsorption isotherms, D3 was a single-layer chemical adsorption,

while D5 and D7 were multilayer chemical adsorption. The adsorption of phenol by biochar may exist π - π interaction, hydrogen bonding, electrostatic adsorption, hydrophobic interaction, and pore filling.

The extracellular polysaccharide of bacteria and its hydrophilic groups were primarily responsible for the adsorption of D7 on bacteria. The combined action of extracellular protein and polysaccharide of bacteria was responsible for the adsorption of the other two types of biochar on bacteria. The hydrophilicity, hydrophobicity and pore size of biochar would affect its fixed biomass. For the strain JH1, the length was about 0.5–1 μm , and the most suitable pore size was 1–5 μm . It was proved that D5 was the best rice husk biochar carrier. Meanwhile, in cycle experiment, the biomass of strain JH1 fixed with D5 was the highest. According to the SEM images of different cycles, with the increase of cycles, bacteria rapidly grew and adhered to biochar, and finally formed thick and sticky biofilms. After the sixth cycle, all the immobilized bacteria of biochar could remove 300 mg/L phenol solution within 12 h. These results indicated that rice husk biochar as a carrier immobilized JH1 had the potential of biological removal of phenol, had the reusability, and showed good stability and durability.

Data availability statement

The datasets presented in this study can be found in online repositories. The names of the repository/repositories and accession number(s) can be found in the article/[Supplementary Material](#).

Author contributions

ML: Conceptualization, Data curation, Methodology, Software, Writing–original draft, Writing–review and editing. JX:

Investigation, Visualization, Writing–review and editing. ZZ: Validation, Writing–review and editing. TZ: Writing–review and editing. YR: Writing–review and editing.

Funding

The author(s) declare financial support was received for the research, authorship, and/or publication of this article. This study was financially supported by National Key R&D Program of China (2020YFC1808803), and the National Natural Science Foundation of China Projects (U21A2003).

Conflict of interest

The authors declare that the research was conducted in the absence of any commercial or financial relationships that could be construed as a potential conflict of interest.

Publisher's note

All claims expressed in this article are solely those of the authors and do not necessarily represent those of their affiliated organizations, or those of the publisher, the editors and the reviewers. Any product that may be evaluated in this article, or claim that may be made by its manufacturer, is not guaranteed or endorsed by the publisher.

Supplementary material

The Supplementary Material for this article can be found online at: <https://www.frontiersin.org/articles/10.3389/fenvs.2023.1294791/full#supplementary-material>

References

- Ahmad, M., Ok, Y. S., Rajapaksha, A. U., Lim, J. E., Kim, B.-Y., Ahn, J.-H., et al. (2016). Lead and copper immobilization in a shooting range soil using soybean stover and pine needle-derived biochars: chemical, microbial and spectroscopic assessments. *J. Hazard. Mater.* 301, 179–186. doi:10.1016/j.jhazmat.2015.08.029
- Amenaghawon, A. N., Anyalewechi, C. L., Okieimen, C. O., and Kusuma, H. S. (2021). Biomass pyrolysis technologies for value-added products: a state-of-the-art review. *Environ. Dev. Sustain.* 23, 14324–14378. doi:10.1007/s10668-021-01276-5
- Amin, M., and Chetpattananondh, P. (2019). Biochar from extracted marine *Chlorella* sp. residue for high efficiency adsorption with ultrasonication to remove Cr(VI), Zn(II) and Ni(II). *Bioresour. Technol.* 289, 121578. doi:10.1016/j.biortech.2019.121578
- Bakina, L. G., Chugunova, M. V., Polyak, Y. M., Mayachkina, N. V., and Gerasimov, A. O. (2021). Bioaugmentation: possible scenarios due to application of bacterial preparations for remediation of oil-contaminated soil. *Environ. Geochem. Health* 43, 2347–2356. doi:10.1007/s10653-020-00755-4
- Balmuk, G., Videgain, M., Manyà, J. J., Duman, G., and Yanik, J. (2023). Effects of pyrolysis temperature and pressure on agronomic properties of biochar. *J. Anal. Appl. Pyrolysis* 169, 105858. doi:10.1016/j.jaap.2023.105858
- Chen, Y., Yu, B., Lin, J., Naidu, R., and Chen, Z. (2016). Simultaneous adsorption and biodegradation (SAB) of diesel oil using immobilized *Acinetobacter venetianus* on porous material. *Chem. Eng. J.* 289, 463–470. doi:10.1016/j.cej.2016.01.010
- Dave, K., and Dhayal, M. (2017). Fluorometric estimation of amino acids interaction with colloidal suspension of FITC functionalized graphene oxide nanoparticles. *Appl. Surf. Sci.* 396, 978–985. doi:10.1016/j.apsusc.2016.11.070
- Du, J., Sun, P., Feng, Z., Zhang, X., and Zhao, Y. (2016). The biosorption capacity of biochar for 4-bromodiphenyl ether: study of its kinetics, mechanism, and use as a carrier for immobilized bacteria. *Environ. Sci. Pollut. Res.* 23, 3770–3780. doi:10.1007/s11356-015-5619-8
- Fan, J., Duan, T., Zou, L., and Sun, J. (2023). Characteristics of dissolved organic matter composition in biochar: effects of feedstocks and pyrolysis temperatures. *Environ. Sci. Pollut. Res.* 30, 85139–85153. doi:10.1007/s11356-023-28431-x
- Frankel, M. L., Bhuiyan, T. I., Veksha, A., Demeter, M. A., Layzell, D. B., Helleur, R. J., et al. (2016). Removal and biodegradation of naphthenic acids by biochar and attached environmental biofilms in the presence of co-contaminating metals. *Bioresour. Technol.* 216, 352–361. doi:10.1016/j.biortech.2016.05.084
- Gai, C., Guo, Y., Peng, N., Liu, T., and Liu, Z. (2016). N-Doped biochar derived from co-hydrothermal carbonization of rice husk and *Chlorella pyrenoidosa* for enhancing copper ion adsorption. *RSC Adv.* 6, 53713–53722. doi:10.1039/c6ra09270e
- Grace Pavithra, K., Sundar Rajan, P., Arun, J., Brindhadevi, K., Hoang Le, Q., and Pugazhendhi, A. (2023). A review on recent advancements in extraction, removal and recovery of phenols from phenolic wastewater: challenges and future outlook. *Environ. Res.* 237, 117005. doi:10.1016/j.envres.2023.117005
- Guo, J., and Chen, B. (2014). Insights on the molecular mechanism for the recalcitrance of biochars: interactive effects of carbon and silicon components. *Environ. Sci. Technol.* 48, 9103–9112. doi:10.1021/es405647e
- Huang, F., Li, K., Wu, R.-R., Yan, Y.-J., and Xiao, R.-B. (2020). Insight into the Cd²⁺ biosorption by viable *Bacillus cereus* RC-1 immobilized on different biochars: roles of bacterial cell and biochar matrix. *J. Clean. Prod.* 272, 122743. doi:10.1016/j.jclepro.2020.122743

- Iqbal, A., Arshad, M., Hashmi, I., Karthikeyan, R., Gentry, T. J., and Schwab, A. P. (2018). Biodegradation of phenol and benzene by endophytic bacterial strains isolated from refinery wastewater-fed *Cannabis sativa*. *Environ. Technol.* 39, 1705–1714. doi:10.1080/09593330.2017.1337232
- Jjagwe, J., Olupot, P. W., Menya, E., and Kalibbala, H. M. (2021). Synthesis and application of granular activated carbon from biomass waste materials for water treatment: a review. *J. Bioresour. Bioprod.* 6, 292–322. doi:10.1016/j.jobab.2021.03.003
- Ke, Q., Zhang, Y., Wu, X., Su, X., Wang, Y., Lin, H., et al. (2018). Sustainable biodegradation of phenol by immobilized *Bacillus* sp. SAS19 with porous carbonaceous gels as carriers. *J. Environ. Manag.* 222, 185–189. doi:10.1016/j.jenvman.2018.05.061
- Keilueit, M., Nico, P. S., Johnson, M. G., and Kleber, M. (2010). Dynamic molecular structure of plant biomass-derived black carbon (biochar). *Environ. Sci. Technol.* 44, 1247–1253. doi:10.1021/es9031419
- Kumar, A., Kumar, S., and Kumar, S. (2005). Biodegradation kinetics of phenol and catechol using *Pseudomonas putida* MTCC 1194. *Biochem. Eng. J.* 22, 151–159. doi:10.1016/j.bej.2004.09.006
- Lehmann, J., Rillig, M. C., Thies, J., Masiello, C. A., Hockaday, W. C., and Crowley, D. (2011). Biochar effects on soil biota—A review. *Soil Biol. Biochem.* 43, 1812–1836. doi:10.1016/j.soilbio.2011.04.022
- Li, J., Jiang, Z., Chen, S., Wang, T., Jiang, L., Wang, M., et al. (2019). Biochemical changes of polysaccharides and proteins within EPS under Pb(II) stress in *Rhodotorula mucilaginosa*. *Ecotoxicol. Environ. Saf.* 174, 484–490. doi:10.1016/j.ecoenv.2019.03.004
- Li, X., Jiang, Y., Chen, T., Zhao, P., Niu, S., Yuan, M., et al. (2023). Adsorption of norfloxacin from wastewater by biochar with different substrates. *Environ. Geochem. Health* 45, 3331–3344. doi:10.1007/s10653-022-01414-6
- Liu, W.-J., Jiang, H., and Yu, H.-Q. (2015). Development of biochar-based functional materials: toward a sustainable platform carbon material. *Chem. Rev.* 115, 12251–12285. doi:10.1021/acs.chemrev.5b00195
- Liu, Y., Gan, L., Chen, Z., Megharaj, M., and Naidu, R. (2012). Removal of nitrate using *Paracoccus* sp. YF1 immobilized on bamboo carbon. *J. Hazard. Mater.* 229–230, 419–425. doi:10.1016/j.jhazmat.2012.06.029
- Lyu, H., Tang, J., Shen, B., and Siddique, T. (2018). Development of a novel chem-bio hybrid process using biochar supported nanoscale iron sulfide composite and *Corynebacterium variabile* HRJ4 for enhanced trichloroethylene dechlorination. *Water Res.* 147, 132–141. doi:10.1016/j.watres.2018.09.038
- Martinková, L., Kotik, M., Marková, E., and Homolka, L. (2016). Biodegradation of phenolic compounds by Basidiomycota and its phenol oxidases: a review. *Chemosphere* 149, 373–382. doi:10.1016/j.chemosphere.2016.01.022
- Mohammadi, S., Kargari, A., Sanaeepur, H., Abbassian, K., Najafi, A., and Mofarragh, E. (2015). Phenol removal from industrial wastewaters: a short review. *Desalination Water Treat.* 53, 2215–2234. doi:10.1080/19443994.2014.883327
- Moussavi, G., Mahmoudi, M., and Barikbin, B. (2009). Biological removal of phenol from strong wastewaters using a novel MSBR. *Water Res.* 43, 1295–1302. doi:10.1016/j.watres.2008.12.026
- Nazos, T. T., Mavroudikis, L., Pergantis, S. A., and Ghanotakis, D. F. (2020). Biodegradation of phenol by *Chlamydomonas reinhardtii*. *Photosynth. Res.* 144, 383–395. doi:10.1007/s11120-020-00756-5
- Palansooriya, K. N., Shaheen, S. M., Chen, S. S., Tsang, D. C. W., Hashimoto, Y., Hou, D., et al. (2020). Soil amendments for immobilization of potentially toxic elements in contaminated soils: a critical review. *Environ. Int.* 134, 105046. doi:10.1016/j.envint.2019.105046
- Panigrahy, N., Priyadarshini, A., Sahoo, M. M., Verma, A. K., Daverey, A., and Sahoo, N. K. (2022). A comprehensive review on eco-toxicity and biodegradation of phenolics: recent progress and future outlook. *Environ. Technol. Innovation* 27, 102423. doi:10.1016/j.eti.2022.102423
- Park, J. H., Ok, Y. S., Kim, S. H., Cho, J. S., Heo, J. S., Delaune, R. D., et al. (2015). Evaluation of phosphorus adsorption capacity of sesame straw biochar on aqueous solution: influence of activation methods and pyrolysis temperatures. *Environ. Geochem. Health* 37, 969–983. doi:10.1007/s10653-015-9709-9
- Pathak, U., Roy, A., Mandal, D. D., Das, P., Kumar, T., and Mandal, T. (2018). Bioattenuation of phenol and cyanide involving immobilised spent tea activated carbon with *Alcaligenes faecalis* JF339228: critical assessment of the degraded intermediates. *Asia-Pacific J. Chem. Eng.* 14, doi:10.1002/apj.2278
- Priyadarshini, A., Mishra, S., Sahoo, N. K., Raut, S., Daverey, A., and Tripathy, B. C. (2023). Biodegradation of phenol using the indigenous rhodococcus pyridinivorans strain PDB9T NS-1 immobilized in calcium alginate beads. *Appl. Biochem. Biotechnol.* doi:10.1007/s12010-023-04508-8
- Qiao, K., Tian, W., Bai, J., Wang, L., Zhao, J., Song, T., et al. (2020). Removal of high-molecular-weight polycyclic aromatic hydrocarbons by a microbial consortium immobilized in magnetic floating biochar gel beads. *Mar. Pollut. Bull.* 159, 111489. doi:10.1016/j.marpolbul.2020.111489
- Ramos-Escobedo, G. T., Pecina-Treviño, E. T., Bueno Tokunaga, A., Concha-Guerrero, S. I., Ramos-Lico, D., Guerra-Balderrama, R., et al. (2016). Bio-collector alternative for the recovery of organic matter in flotation processes. *Fuel* 176, 165–172. doi:10.1016/j.fuel.2016.02.018
- Rushing, J., and Santoro, N. (2022). Current opinion in endocrine and metabolic research perimenopause: utility of testing. *Curr. Opin. Endocr. Metabolic Res.* 27, 100402. doi:10.1016/j.coemr.2022.100402
- Rutherford, D. W., Wershaw, R. L., Rostad, C. E., and Kelly, C. N. (2012). Effect of formation conditions on biochars: compositional and structural properties of cellulose, lignin, and pine biochars. *Biomass Bioenergy* 46, 693–701. doi:10.1016/j.biombioe.2012.06.026
- Sekaran, G., Karthikeyan, S., Gupta, V. K., Boopathy, R., and Maharaja, P. (2013). Immobilization of *Bacillus* sp. in mesoporous activated carbon for degradation of sulphonated phenolic compound in wastewater. *Mater. Sci. Eng. C* 33, 735–745. doi:10.1016/j.msec.2012.10.026
- Shahryari, S., Zahiri, H. S., Haghbeen, K., Adrian, L., and Noghabi, K. A. (2018). High phenol degradation capacity of a newly characterized *Acinetobacter* sp. SA01: bacterial cell viability and membrane impairment in respect to the phenol toxicity. *Ecotoxicol. Environ. Saf.* 164, 455–466. doi:10.1016/j.ecoenv.2018.08.051
- Shen, L. A., Yu, W., Li, L., Zhang, T., Abshir, I. Y., Luo, P., et al. (2021). Microorganism, carriers, and immobilization methods of the microbial self-healing cement-based composites: a review. *Materials* 14, 5116. [Online]. doi:10.3390/ma14175116
- Shen, Z., Zhang, Y., Mcmillan, O., Jin, F., and Al-Tabbaa, A. (2017). Characteristics and mechanisms of nickel adsorption on biochars produced from wheat straw pellets and rice husk. *Environ. Sci. Pollut. Res.* 24, 12809–12819. doi:10.1007/s11356-017-8847-2
- Singh, B. (2018). “13 - rice husk ash,” in *Waste and supplementary cementitious materials in concrete*. Editors R. Siddique and P. Cachim (Woodhead Publishing), 417–460.
- Şolpan, D., Ibrahim, K. E. A., Torun, M., and Mehrnia, M. (2020). The effect of ozonation on the degradation of carbaryl in aqueous solution. *J. Environ. Sci. Health, Part B* 55, 929–939. doi:10.1080/03601234.2020.1798174
- Sun, K., Kang, M., Zhang, Z., Jin, J., Wang, Z., Pan, Z., et al. (2013). Impact of deashing treatment on biochar structural properties and potential sorption mechanisms of phenanthrene. *Environ. Sci. Technol.* 47, 11473–11481. doi:10.1021/es4026744
- Takaoka, M., Yokokawa, H., and Takeda, N. (2007). The effect of treatment of activated carbon by H₂O₂ or HNO₃ on the decomposition of pentachlorobenzene. *Appl. Catal. B Environ.* 74, 179–186. doi:10.1016/j.apcatb.2007.02.009
- Toh, R. H., Lim, P. E., Seng, C. E., and Adnan, R. (2013). Immobilized acclimated biomass-powdered activated carbon for the bioregeneration of granular activated carbon loaded with phenol and o-cresol. *Bioresour. Technol.* 143, 265–274. doi:10.1016/j.biortech.2013.05.126
- Tong, Y., Mcnamara, P. J., and Mayer, B. K. (2019). Adsorption of organic micropollutants onto biochar: a review of relevant kinetics, mechanisms and equilibrium. *Environ. Sci. Water Res. Technol.* 5, 821–838. doi:10.1039/c8ew00938d
- Usman, M., Ren, S., Ji, M., O-Thong, S., Qian, Y., Luo, G., et al. (2020). Characterization and biogas production potentials of aqueous phase produced from hydrothermal carbonization of biomass – major components and their binary mixtures. *Chem. Eng. J.* 388, 124201. doi:10.1016/j.cej.2020.124201
- Wang, L., Wang, Y., Ma, F., Tankpa, V., Bai, S., Guo, X., et al. (2019). Mechanisms and reutilization of modified biochar used for removal of heavy metals from wastewater: a review. *Sci. Total Environ.* 668, 1298–1309. doi:10.1016/j.scitotenv.2019.03.011
- Wang, W., Wang, L., Zhang, M., Yu, B., Li, X., and Yan, H. (2023). Contribution evaluation of physical hole structure, hydrogen bond, and electrostatic attraction on dye adsorption through individual experiments. *Adsorpt. Sci. Technol.* 2023, 1–12. doi:10.1155/2023/4596086
- Wang, X., Wang, X., Liu, M., Bu, Y., Zhang, J., Chen, J., et al. (2015). Adsorption-synergic biodegradation of diesel oil in synthetic seawater by acclimated strains immobilized on multifunctional materials. *Mar. Pollut. Bull.* 92, 195–200. doi:10.1016/j.marpolbul.2014.12.033
- Wu, M., Li, J., Zhi, Y., van de Vosse, F. N., Janssen, R. P. A., van Donkelaar, C. C., et al. (2021). Spectroscopic photoacoustic imaging of cartilage damage. *J. Agro-Environment Sci.* 40, 1071–1080. doi:10.1016/j.joca.2021.04.001
- Xiao, X., Chen, B., and Zhu, L. (2014). Transformation, morphology, and dissolution of silicon and carbon in rice straw-derived biochars under different pyrolytic temperatures. *Environ. Sci. Technol.* 48, 3411–3419. doi:10.1021/es405676h
- Yang, K., Li, H., Xia, Y., Li, H., and Chang, H. (2019). Experimental research on performance of flexible polypropylene-fiber and modified emulsion-asphalt mixture. *J. Mater. Sci. Eng.* 37, 138–143. doi:10.14136/j.cnki.issn1673-2812.2019.01.025
- Yao, F., Liu, D., Zhang, J., and Wang, P. (2016). Estimation of rice yield with a process-based model and remote sensing data in the middle and lower reaches of yangtze river of China. *J. Indian Soc. Remote Sens.* 45, 477–484. doi:10.1007/s12524-016-0596-z
- Yu, Y., An, Q., Zhou, Y., Deng, S., Miao, Y., Zhao, B., et al. (2019). Highly synergistic effects on ammonium removal by the co-system of *Pseudomonas stutzeri* XL-2 and modified walnut shell biochar. *Bioresour. Technol.* 280, 239–246. doi:10.1016/j.biortech.2019.02.037
- Yu, Y., Guo, H., Zhong, Z., Lu, Z., Zhu, X., Li, Z., et al. (2023). Enhanced removal of tetrabromobisphenol A by *Burkholderia cepacia* Y17 immobilized on biochar. *Ecotoxicol. Environ. Saf.* 249, 114450. doi:10.1016/j.ecoenv.2022.114450

Zeng, Q., Xu, J., Hou, Y., Li, H., Du, C., Jiang, B., et al. (2021). Effect of Fe₃O₄ nanoparticles exposure on the treatment efficiency of phenol wastewater and community shifts in SBR system. *J. Hazard. Mater.* 407, 124828. doi:10.1016/j.jhazmat.2020.124828

Zhang, J., Li, J., Ye, D., Zhu, X., Liao, Q., and Zhang, B. (2014). Tubular bamboo charcoal for anode in microbial fuel cells. *J. Power Sources* 272, 277–282. doi:10.1016/j.jpowsour.2014.08.115

Zhang, L., Dong, L., and Xuepingyang. (2019). Phenol production technology progress and market analysis. *Technol. Econ. Petrochem.* 35, 24–28. doi:10.3969/j.issn.1674-1099.2019.05.006

Zhao, L., Xiao, D., Liu, Y., Xu, H., Nan, H., Li, D., et al. (2020). Biochar as simultaneous shelter, adsorbent, pH buffer, and substrate of *Pseudomonas*

citronellolis to promote biodegradation of high concentrations of phenol in wastewater. *Water Res.* 172, 115494. doi:10.1016/j.watres.2020.115494

Zhao, X., Wang, J., Fang, L., Tang, Z., and Wu, A. (2019). Research advances on the aggregation and sedimentation of synthetic nanomaterials in the aquatic environment. *Bull. Mineralogy, Petrology Geochem.* 38, 522–533. doi:10.1016/j.watres.2020.115494

Zheng, J., Zhang, J., Gao, L., Wang, R., Gao, J., Dai, Y., et al. (2021). Effect of straw biochar amendment on tobacco growth, soil properties, and rhizosphere bacterial communities. *Sci. Rep.* 11, 20727. doi:10.1038/s41598-021-00168-y

Zhu, F. (2018). Interactions between cell wall polysaccharides and polyphenols. *Crit. Rev. Food Sci. Nutr.* 58, 1808–1831. doi:10.1080/10408398.2017.1287659